Integration of SMRs with Steel Industry

by David Carlsén

LUND
UNIVERSITY

Thesis for the degree of Master of Science

Thesis advisors:
Magnus Genrup, Lund University
Balder Hagert and Simon Wakter, AFRY

To be presented, with the permission of the Faculty of Engineering of Lund University, for public criticism
at the Department of Energy Sciences on Friday the 14th of October 2022 at 08:30.

This degree project for the degree of Master of Science in Engineering has been conducted at the Division of Thermal Power Engineering, Department of Energy Sciences, Faculty of Engineering, Lund University. Besides, it has been carried out in cooperation with AFRY and their Nuclear Division.

Supervisor at Lund University was Magnus Genrup, Professor in Thermal Power Engineering and Department Head of the Department of Energy Sciences. Supervisor at AFRY was first Simon Wakter and then Balder Hagert. Examiner at Lund University was Marcus Thern, Senior lecturer in Thermal Power Engineering.

Many thanks to Ola Wallberg, Professor and Department Head at the Department of Chemical Engineering, Lund University, for providing invaluable input regarding chemistry. Also thanks to Staffan Qvist, Energy Engineer with a Ph.D. in Nuclear Engineering, for giving an introduction to nuclear steelmaking systems. Lastly, special thanks to my brother Edvin Carlsén, student in Environmental Engineering, for valuable discussions regarding thermodynamics.

Department of Energy Sciences
Faculty of Engineering
Lund University

ISSN: <0282-1990>
LUTMDN/TMHP-22/5509-SE

Typeset in LaTeX
Lund 2022

Contents

List of Figures

List of Tables

Nomenclature

Abbreviations

BF-BOF Blast Furnace-Basic Oxygen Furnace

BPT Back Pressure Turbine

CCU Carbon Capture and Utilization

DAC Direct Air Capturing

DRI Directly Reduced Iron

DRP Direct Reduction Plant

EAF Electric Arc Furnace

EL-DRP-EAF Electrolysis-Direct Reduction Plant-Electric Arc Furnace

GHG Greenhouse Gases

HPT High Pressure Turbine

LHV Lower Heating Value

LPT Low Pressure Turbine

LTE Low Temperature Electrolysis

RES Renewable Energy Sources

SMR Small Modular Reactor

SOEC Solid Oxide Electrolysis Cell

TTD Terminal Temperature Difference

VHTR Very High Temperature Reactor

Abstract

The steel industry is with its high emissions an important sector to transform from fossil-fueled to fossil-free. In recent years, the technology development has accelerated quickly regarding iron ore reduction using hydrogen produced from electrolysis within the EL-DRP-EAF steel production route. However, it is problematic that the energy supply for the majority of the efforts made within the green transition, steel production included, is to come from electricity. In this study it is investigated if it is possible to reduce the primary energy demand of the EL-DRP-EAF route by using direct heat integration of hot SMR steam into the process. A beneficial design of such a system is proposed and later on modeled in order to find out how much SMR steam that is needed to produce 1 ton of DRI. It is found that the primary energy demand can be reduced compared to other systems, with direct heat integration of hot SMR steam as what makes the difference. Though, the result is sensitive to somewhat unsimilar assumptions and system boundaries of the compared modelings. Lastly, scaling of the system result is performed based on the Swedish DRI production rate. As the energy demand is vast, the suggestion is made that the nearby located SMRs could be used for direct heat integration only, whilst the remaining energy demand in the form of electricity could be taken from the grid. That would allow for a mix of energy sources and still lead to the reduction in energy demand.

Chapter 1

Introduction

1.1 Background

IPCC states in their latest report that climate change caused by anthropogenic activities is one of the largest issues for the future of the planet [1]. Rising sea levels, increased global temperature, extinction of species, more extreme weather and droughts are only a few of the upcoming and ongoing events to be concerned about. A rapid decrease in the concentration of atmospheric GHG is needed if earth is going to be a place where its current inhabitants, including humans, are to live with a similar quality of life as today. Unfortunately, things are not moving in the right direction. GHG emissions are still increasing as well as the overall concentration in the atmosphere.

A key aspect in reducing climate change is the green energy transition with the abandonment of fossil fuels [1]. Industries are responsible for 31 % of the annual global CO_2 emissions [2]. Thus, the transition of high-emitting industries from fossil-fueled to fossil-free will have a great impact on worldwide emissions. The steel industry is such an example since it constitutes 7 % of the world's GHG emissions [3]. Steel is a widely used material for construction, transport etc. In 2021, 1.951 billion tonnes was produced globally and the demand for it is higher than ever before [4]. This increasing trend is likely to continue [5]. In Sweden, where 87.4 % of the iron ore was mined in the EU in 2020 [4], as much as 12-13 % of the yearly total GHG emissions come from the steel industry [6]. Thus, this is an important sector to transform if the GHG emissions are to decrease.

Steel is today mainly manufactured through the so-called BF-BOF production route. Firstly, iron ore (mined as either hematite Fe_2O_3 or magnetite Fe_3O_4) is reduced to crude iron in a blast furnace using coking coal as reducing agent. This process is one of the main causes for the steel industry's massive CO_2 emissions. Secondly, the crude iron is processed in a basic oxygen furnace along with alloying elements in order to purify and strengthen the end product, steel [7].

As part of the green energy transition, new research projects such as HYBRIT are developing methods in which the coking coal can be replaced with H_2 as a reducing

agent. This technology results in almost zero CO_2 emissions if the H_2 is produced from water electrolysis running on fossil-free electricity. Here, the iron ore is firstly reduced to DRI using H_2 in a so-called DRP and then further refined into steel in an EAF [8]. Clear is that this EL-DRP-EAF route is considered to be the most promising concept today [2] [8] [9]. The DRP is actually a highly used process on industrial scale already, but mostly with the usage of methane as a reducing agent. But already in the 1990s, it was demonstrated on an industrial scale that the process can be run with hydrogen as a reducing agent instead, with similar result. Since this initial concept proof it took quite some time until very recent years before the technology development started to accelerate within the EL-DRP-EAF route [8].

There are a few articles written until today about the EL-DRP-EAF route. From 2018 and onwards, the article written by Vogl, Åhman and Nilsson and the article by Bhaskar, Assadi and Somehsaraei started by presenting detailed process designs and model those with basis in mass- and energy balance calculations [10] [3]. Both used LTE with electrical heating afterwards to provide the DRP with hydrogen at the high temperature that is needed. After this, Müller et al. (hereafter denoted as project A) presented a critical review of those two, stating that they have made several substantial assumptions in their modeling, especially when not considering energy balances within the DRP [8]. Therefore, project A presented an improved extensive model of the route, considering not only LTE but also high temperature SOEC [8]. That work has many similarities to what Krüger et al. (hereafter denoted as project B) presented shortly afterwards [11]. Both projects A and B showed that usage of SOEC over LTE has the potential to reduce the primary energy demand of steel production due to the possibilities of introducing waste heat integration and by-product utilization when using SOEC. But, non of them introduced direct heat integration of external heat for the remaining energy demand, only electrical heating, despite both indicating that direct heat integration should lead to a further minimized overall energy demand of steel production.

It is problematic that the energy supply for the majority of the efforts made within the green transition is to come from electricity. HYBRIT, focusing mostly on LTE and electrical heating in their system development so far, announces that 55 TWh of electricity will be needed in total for their supply when operating in full scale [12]. That can be compared to the total electricity production in Sweden of 166 TWh in 2021 [13]. Meanwhile, there are numerous other transition projects going on, many of them involving hydrogen as an intermediate energy carrier, that will require even more electricity in the future. That makes the electricity supply a very critical aspect for the fossil-free industry transition to become reality.

As stated by scientists, industry leaders and governmental authorities, all kinds of fossil-free energy sources will be needed if we are to succeed with the transition [14]. But most transition projects focus on electrical energy supply from RES. In northern Sweden, where the mines are located, they have a good reason for doing so as the RES potential is great. Certainly, with some of the lowest electricity prices in Europe these days. But also the perspective of being able to store energy in the form of hydrogen

makes fossil-free steel production fueled by RES an interesting option, as hydrogen energy storage can help with providing grid stability in an energy system with large shares of intermittent RES. But still, despite all that, the electricity demand for steel production is tremendous. Also, large amounts of heat is needed on a constant basis. Furthermore, both projects A and B indicated that direct heat integration might lead to minimized overall energy demand of steel production [8] [11]. From that reasoning, the idea behind this thesis came up. What if we combine steel production with very high temperature SMRs? There should be some overall efficiency advantages if benefiting from the SMR steam directly into the steel production process, without having to go from hot steam, to electricity, to heat again and in that way losing overall efficiency.

As mentioned, recent projects have put focus into using electricity for supplying the fossil-free steel process with energy. But there have actually been some projects going on earlier, especially in Japan, regarding directly supplying the steel industry with nuclear energy, starting already in the 1960s [15]. The development continued in later days until 2014 when it was ended as a result of the Fukushima incident [15] [16] [17] [18]. A nuclear steelmaking system with the Japanese VHTR (950 °C helium output) was considered as very promising and competitive [15] [16]. However, the previous Japanese research was based on a iodine-sulfur process for hydrogen production [15] [16] [18], which today is not as promising as SOEC due to the drastic escalation in the development of SOEC in recent years [19] [20]. Thus, this study will contribute with new perspectives in providing a nuclear steelmaking system, with usage of the newest technologies out there.

1.2 Purpose

The main goal of this project is to investigate if it is possible to reduce the primary energy demand of fossil-free steel production by using direct heat integration of hot SMR steam in the process. In order to fulfill this goal, the following underlying questions have been researched:

- Which type of SMR is suitable to supply the energy demand in the form of heat, hydrogen and electricity?
- What can a system design, incorporating SMR steam into the steel process in a beneficial way, look like?
- How much SMR steam is needed to produce 1 ton of DRI with that system design?
- Is that energy demand of SMR steam lower if compared to the energy demand of already existing system suggestions?
- In what ways could SMRs be reasonably integrated with the steel industry in a real scale?

1.3 Delimitations

This work was performed out of an energy efficiency perspective. Analysis of cost and emissions were dismissed. The emissions are already known as almost negligible compared to today's BF-BOF route. Therefore, in order to minimize the world's emissions, it is seen as more important now to put focus into actually realizing the EL-DRP-EAF route to an as large extent as possible. A minimized overall energy demand of the EL-DRP-EAF route likely increases the probability of it becoming reality in larger scale across the world.

The only components of the EL-DRP-EAF route that were included in this work are the DRP and SOEC. This choice was made based on that the electrolysis by far has the largest energy demand of the components throughout the system [3]. It's therefore most interesting to study from an energy supply perspective as the impact can be greatest here. Both the DRP and the SOEC have to be in the same location geographically seen in order to be able to perform heat integration of SMR steam into the processes.

Thus firstly, the initiating iron ore mining and pelletizing process were excluded. In the pelletizing, magnetite Fe_3O_4 is oxidized to hematite Fe_2O_3 [21]. So, this work focused on hematite iron ore only. In Sweden, magnetite is the most common type of iron ore but globally hematite is more abundant [21]. Therefore, pelletizing is relevant for the LKAB process, but not in a global perspective. Additionally, the pelletizing is very seldom situated on the same spot as the iron ore reduction [22], which in all those cases makes it impossible to integrate SMR steam for both pelletizing and DRP+SOEC anyways.

Thus secondly, the finishing EAF was excluded. It is most commonly the case that the ironmaking takes place in one location and that the iron then is shipped away to produce the desired final steel products in another location.

No optimization was performed when developing the system design. Instead, well-motivated choices of the individual components, as well as how they are connected, were made in order to come up with one promising system design.

As LKAB, the Swedish mining company behind the market leading HYBRIT initiative, have announced that their production is to become totally carbon free in 2045 [23], this study only considered technologies that are very likely to be on the market in industrial scale in 2035. Thus, allowing for 10 years of construction time.

This project did not analyze the possible advantages with SMRs before conventional nuclear power plants. Anyway, the aim is to investigate the possibilities of supplying the steel industry with energy from SMRs, not to make a comparison of SMRs to conventional nuclear power plants.

No thorough calculations were performed of the pulp of either the DRP or SMR. These two system components were only seen as black boxes for the modeling, using already specified input and output data.

This work did not dig deeply into different nuclear reactor technologies as the focus was set on an overall energy efficiency perspective, seeing the SMR as a black box. No analysis or discussion of the full nuclear power plant life cycle, e.g. fuel production and radioactive waste storage solutions, was performed. That includes ethical, political and safety aspects. No discussion was written regarding the likeliness of a SMR steelmaking system actually being put into place, thinking of e.g. regulations that have to be updated to allow for SMRs.

Even though the SMRs and SOEC can generate a relatively stable supply of H_2 to the DRP, it is hard to match the demand exactly. A smaller H_2 storage would in reality be needed here in between but that was excluded in this work. Also production and storage of the CO_2 that must be added to the process to compensate for the carbon addition to the DRI was excluded.

Sulfur species originating from the iron ore might be present in the DRP outlet gas. Sulfur can reduce the quality of the produced steel and deactivate the nickel-catalyst used in SOEC, so those need to be removed before recirculating the outlet DRP gases. There are many commercial solutions available [11]. However, this was not included.

No profound study of gas separation technologies was made in this project. That holds especially for the separation of CO_2 and inert gases.

1.4 Project Outline

Chapter 2 presents the used thermodynamic quantities and equations firstly. Then comes a technical description of the individual technologies used to build up the system.

Chapter 3 contains one method and one result section regarding the proposed system design. The method section describes how the system design was established. The result section presents the proposed system in the form of a schematic together with details, including the assumptions made in order to come up with the system.

Chapter 4, also containing one method and one result section, regards the modeling of the proposed system design. The method section describes the modeling calculations, including the modeling-related assumptions. The result section presents how much SMR steam that is needed to produce 1 ton of DRI with the proposed system, together with further scaled details of the modeling result.

Chapter 5 contains a discussion regarding this project.

Chapter 6 concludes the study as well as highlights areas that could be of interest for future studies.

Chapter 2

Theory

2.1 Thermodynamics

In order to be able to design a system where SMR steam is integrated in fossil-free steel production it is first of all necessary to have a basic understanding of relevant thermodynamics. The first law of thermodynamics states that the rate of change in energy for a defined system is

$$\dot{E}_{\text{sys}} = \dot{E}_{\text{in}} - \dot{E}_{\text{out}} \tag{2.1}$$

where $\dot{E}_{\text{in}}$ and $\dot{E}_{\text{out}}$ are the energy flows in and out. This is derived from the conservation law which says that energy can only be transformed, not created or destroyed. More specifically, it holds that for a sum of substances

$$\dot{E}_{\text{sys}} = \Sigma(\dot{Q} + \dot{W} + \dot{m}h)_{\text{in}} - \Sigma(\dot{Q} + \dot{W} + \dot{m}h)_{\text{out}} \tag{2.2}$$

where $\dot{Q}$ is the heat flow, $\dot{W}$ the work flow, $\dot{m}$ the mass flow and h the specific enthalpy of each substance. For a very simple thermodynamic process, such as the splitting of one stream into two, $\dot{Q}$ and $\dot{W}$ are practically zero. Furthermore, it holds that $\dot{E}_{\text{in}} = \dot{E}_{\text{out}}$, resulting in that $\dot{E}_{\text{sys}}$ is zero according to equation 2.1. Thus, what is left from equation 2.2 is only

$$\Sigma(\dot{m}h)_{\text{in}} = \Sigma(\dot{m}h)_{\text{out}}. \tag{2.3}$$

Enthalpy H is a state function of a thermodynamic system which is defined as

$$H = U + pV \tag{2.4}$$

where U is the system's internal energy, p its pressure and V its volume. As U does not take the system's physical dimensions into account, the term pV is used as a measure of how much the system displaces its surroundings. The equation

$$dH = C_p dT - C_p \mu_{\text{JT}} dp \tag{2.5}$$

describes how the enthalpy changes with p and temperature T. C_p is the specific heat

capacity. Worth noting is that during isobaric conditions, the Joule-Thomson effect, represented by μ_{JT}, can be neglected as dp is zero.

When using tabular values, it is important to consider that the enthalpies consist of two parts. One part is the standard enthalpy of formation H_F, defined for 25 °C and 1 bar, which is zero for each element in its most thermodynamically stable form. It is negative for substances that are even more stable and positive for less stable substances. Tabular values of H_F can be found in *Atkins' Physical Chemistry* [24]. The remaining part is the contribution from changes in T and p with respect to a reference state, following equation 2.5. Some programs, such as ASPEN, consider both parts in their enthalpy values, while others, such as REFPROP, only consider the contribution from changes in T and p.

Also worth noting is that it is important to use the same tabular in REFPROP for each substance all the way through the calculations, as different tabulars differ slightly from each other. Furthermore, when having mixtures of substances, it affects the chemical potential. Therefore, it is not as simple as taking a mass-weighted mean value of the substances' own enthalpies. But REFPROP can provide values both for pure substances and mixtures. REFPROP takes activity factors and chemical potential into account when providing combined enthalpy values for mixtures, which makes those values beneficial to use directly.

For a chemical reaction, a total enthalpy difference ΔH can be determined by subtracting the sum of the reactants' enthalpy from the sum of the products' enthalpy as shown by

$$\mathrm{A} + \mathrm{B} \longrightarrow \mathrm{C} + \mathrm{D} \tag{2.I}$$

$$\Delta H = (H_C + H_D) - (H_A + H_B) \tag{2.6}$$

where a negative value of ΔH means that the reaction is exotherm and a positive value implies an endotherm reaction. Here, it is important to include both H_F and the p-T-dependent part of the H tabular values, to account for the different substances and that the reaction occurs at a certain p-T state.

Continuing with chemical reactions, another important concept to grasp is Gibbs free energy, G. It can be seen as a thermodynamic potential represented by the maximum measure of work that a closed system can carry out at constant pressure and temperature [25]. If the Gibbs free energy in a system is zero, it implies that the system is in a thermodynamic equilibrium. If the change in Gibbs free energy ΔG for a reaction is less than zero, it means that the reaction may occur spontaneously. On the contrary, if ΔG is higher than zero, that amount of activation energy is needed to be supplied for the reaction to take place. ΔG of a chemical reaction occurring at a certain p-T state is calculated by

$$\Delta G = \Delta H - T\Delta S \tag{2.7}$$

with usage of ΔH as per before. ΔS is the change in entropy at the reaction's p-T state, calculated similarily to as in equation 2.6. Again, comparable to H, also S has two parts of its tabular values. The first part is the standard molar entropy S^0, defined in *Atkins'*

Physical Chemistry as the entropy content of one mole of pure substance at a standard state of 25 °C and 1 bar [24]. The remaining part is the p-T-dependent part which can be obtained from REFPROP in a correct way if setting the reference state to 25 °C and 1 bar.

2.2 Heat Exchangers

Firstly in this section comes a description of how to calculate the outcome of a countercurrent heat exchanger when none of the two fluids is undergoing a phase transformation. Secondly comes a similar description but for when one of the fluids is undergoing a phase transformation while being heat exchanged.

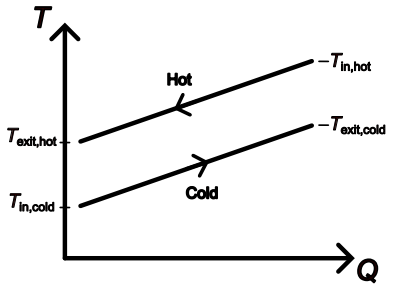

Figure 2.1: T-Q-diagram of a countercurrent heat exchanger with no phase transformation.

Looking at the T-Q-diagram of a commonly used countercurrent heat exchanger, presented in figure 2.1, it is seen how the hot and cold fluid flow countercurrent. The inlet and exit temperatures are denoted. To calculate this, two variables used for simplifying the calculations are presented for the hot and cold stream respectively

$$c_{\text{cold}} = \dot{n}_{\text{cold}} C_{p,\text{cold}} \tag{2.8}$$

$$c_{\text{hot}} = \dot{n}_{\text{hot}} C_{p,\text{hot}} \tag{2.9}$$

where $\dot{n}$ is the molar flow and C_p the specific heat capacity (molar-based).

The heat exchanger's efficiency η is defined as

$$\eta = \frac{\dot{Q}}{\dot{Q}_{\max}} \tag{2.10}$$

where $\dot{Q}_{\max}$ is defined as

$$\begin{aligned} \dot{Q}_{\max} = \min(c_{\text{cold}}(T_{\text{in,hot}} - T_{\text{in,cold}}),\ c_{\text{hot}}(T_{\text{in,hot}} - T_{\text{in,cold}})) = \\ \min(c_{\text{cold}},\ c_{\text{hot}})(T_{\text{in,hot}} - T_{\text{in,cold}}) = c_{\min}(T_{\text{in,hot}} - T_{\text{in,cold}}) \end{aligned} \tag{2.11}$$

and $\dot{Q}$ as

$$\dot{Q} = c_{\text{cold}}(T_{\text{exit,cold}} - T_{\text{in,cold}}) = c_{\text{hot}}(T_{\text{exit,hot}} - T_{\text{in,hot}}). \tag{2.12}$$

That results at last in an equation from where two unknowns can be obtained:

$$\eta = \frac{c_{\text{cold}}(T_{\text{exit,cold}} - T_{\text{in,cold}})}{c_{\text{min}}(T_{\text{in,hot}} - T_{\text{in,cold}})} = \frac{c_{\text{hot}}(T_{\text{exit,hot}} - T_{\text{in,hot}})}{c_{\text{min}}(T_{\text{in,hot}} - T_{\text{in,cold}})}. \tag{2.13}$$

A common η value for a countercurrent plate heat exchanger is 90 % [26].

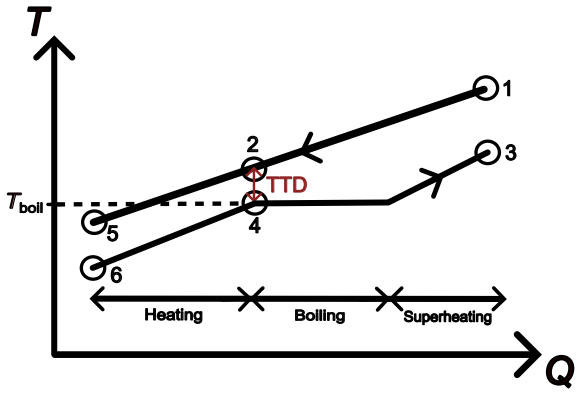

Figure 2.2: T-Q-diagram of a countercurrent heat exchanger with phase transformation.

Now looking at the T-Q-diagram in figure 2.2, a phase transformation of the cold fluid is seen. The boiling temperature T_{boil} can be obtained from REFPROP for a certain pressure of the fluid by setting the fluid quality to in between 0 (saturated liquid) and 1 (saturated gas). For this case of heat exchanging, instead of defining an efficiency η in percent, the efficiency-related TTD number can be used. Is is defined as the temperature difference between points 2 and 4. Smaller TTD means higher efficiency. Having taken the TTD into account, it holds that

$$\Delta Q_{\text{hot}} = \Delta Q_{\text{cold}} \tag{2.14}$$

from which the desired quantities can be obtained.

2.3 DRP

The DRP is the part of the fossil-free steel process that reduces the iron ore (Fe_2O_3) to DRI (Fe). The iron ore falls downwards via gravity, while the hot reducing gases flow upwards [11]. As mentioned in section 1.1, thorough modelings of the EL-DRP-EAF route have already been made in projects A and B [8] [11]. Furthermore, a profound modeling of the DRP itself was performed by Yi et al. [27]. In this section, their result regarding the DRP is put together. At the end, the DRP parameters used in project B are

gathered in table 2.1 to be used as a black box for the modeling performed in this work. As neither project A nor Yi et al. specified enough of its used DRP parameters, those are not included in the table.

The chemical reaction for hydrogen-based reduction of iron ore is

$$Fe_2O_3 + 3H_2 \longrightarrow 2Fe + 3H_2O \qquad \Delta H^0 = 98.0 \text{ kJ/mol}. \tag{2.II}$$

As H^0 is positive for the reference state, it is an endothermic reaction. The reduction of iron ore can also take place by using CO as reducing agent. That chemical reaction is

$$Fe_2O_3 + 3CO \longrightarrow 2Fe + 3CO_2 \qquad \Delta H^0 = -23.6 \text{ kJ/mol}, \tag{2.III}$$

thus an exothermic reaction. Thus, if the DRP is run on CO instead of H_2, the energy demand can be reduced [8].

If one considers more aspects, the situation becomes more complex. These aspects have to be weighed against each other in order to come up with an optimal H_2:CO (syngas) ratio. One aspect is that the energy demand of separating the outlet gases in order to avoid CO_2 emissions increases with larger shares of CO [8] [11]. This effect prevails the advantage of CO reduction being exothermic, at least for the system design used in project A, which makes that the overall energy demand increases when the H_2:CO ratio decreases [8]. Another aspect pointing in this direction is that an increased H_2:CO ratio leads to an increased reduction rate of the iron ore, something that is desirable. When the H_2:CO ratio increases from 0.4 to 1.6, the increase in reduction rate is significant. Between 1.6 and 2.6, the reduction rate stays invariant [27].

But still, despite these aspects, operation with syngas is considered as advantageous [8]. When using syngas, some amount of the carbon gets added to the produced DRI, typically as cementite Fe_3C in a very exothermic reaction [11]. Having carbon in the DRI reduces the electricity demand later on in the EAF [3] [8] [11]. The DRI should optimally contain 3-4.5 mass% coal to match the requirements considering that the right amount of carbon addition to the final steel product makes it obtaining its desired properties [28]. Furthermore, if the syngas is produced from co-electrolysis of H_2O and CO_2, the DRP process acts like a carbon sink where CO_2 can be taken e.g. from the air using DAC and added to the DRI. This results in a further emission reduction compared to using only H_2. It is a fossil-free manner of introducing carbon to the DRI [8] [11].

The DRP modeling of project B was performed for a carbon addition to the DRI of 1 mass%. Its used DRP inlet H_2:CO ratio was 2.0 [11].

It is important to keep a high temperature within the DRP for the iron ore reduction to occur. Raising temperature can effectively raise the reduction rate, but if the temperature becomes too high (over 1000 °C) the reduction rate is significantly slowed. An optimal reduction temperature is 950 °C [27]. However, both projects A and B used 900 °C as temperature of the DRP inlet reduction gases as they also accounted for the possibility of

inserting the reduction gases produced in the SOEC at 900 °C directly into the DRP at that temperature, not having to heat the reduction gases any further [8] [11]. In project A, an outlet DRI temperature of 600-700 °C was obtained for a non-specified inlet iron ore temperature [8]. In project B, 850 °C DRI was obtained for 25 °C inlet iron ore [11]. Outlet gas temperature was 400-450 °C in project A [8] and 464 °C in project B [11].

Around 30 mol% of the reduction gases (both H_2 and CO) react with the iron ore [27]. This number was later on used also for the modelings done in projects A and B [8] [11]. It is clearly unsought to emit the DRP outlet gases. Those can instead advantageously be recirculated and reused in the SOEC, as proven in the following section 2.4. Nevertheless, 10 % of the outlet DRP gases have to be combusted in order to avoid accumulation of inert gases in the system. But also from here it is desirable to separate and recirculate the CO_2 from the combustion in order to avoid emissions [11].

Table 2.1: The properties of the DRP modeling done in project B [11].

Inlet gas temp	900 °C	Inlet gas molar flow	98.4 kmol/tDRI	Outlet gas molar flow	97.6 kmol/tDRI
Outlet gas temp	464 °C	Inlet gas H_2	56.9 mol%	Outlet gas H_2	40.2 mol%
Inlet iron ore temp	25 °C	Inlet gas CO	28.5 mol%	Outlet gas CO	18.4 mol%
Outlet DRI temp	850 °C	Inlet gas CO_2	4.1 mol%	Outlet gas CO_2	13.6 mol%
H2 and CO that react	30 %	Inlet gas H_2O	10.3 mol%	Outlet gas H_2O	27.6 mol%
DRI carburization rate	1 wt%	Inlet gas CH_4	0.14 mol%	Outlet gas CH_4	0.14 mol%
Inlet gas pressure	2 bar				
Outlet gas pressure	1 bar				

2.4 SOEC

Electrolysis is in general a technique that uses direct electrical current to drive an otherwise non-spontaneous chemical reaction. Water electrolysis is perhaps the most well-known example, with reaction

$$H_2O \longrightarrow H_2 + 1/2\, O_2 \qquad \Delta H^0 = 286 \text{ kJ/mol}. \tag{2.IV}$$

Also splitting of CO_2 is possible using electrolysis, with reaction

$$CO_2 \longrightarrow CO + 1/2\, O_2 \qquad \Delta H^0 = 283 \text{ kJ/mol}. \tag{2.V}$$

In figure 2.3 it can be seen how the three terms of equation 2.7 vary as a function of electrolysis temperature, for both H_2O and CO_2 electrolysis. Keeping equation 2.7 in mind, ΔG here corresponds to the electricity supply needed to convert 1 mol of reactant. It can clearly be seen that ΔG decreases with increasing temperature. Moreover, note that for the temperature interval in which SOEC operates, 750-900 °C, ΔG of H_2O and CO_2 is somewhat equal. That is what makes it possible to run SOEC on syngas, as having

that amount of electricity supply makes both reactions occur. Hence, it is possible to produce H_2 and CO at 900 °C, to be inserted directly into the DRP.

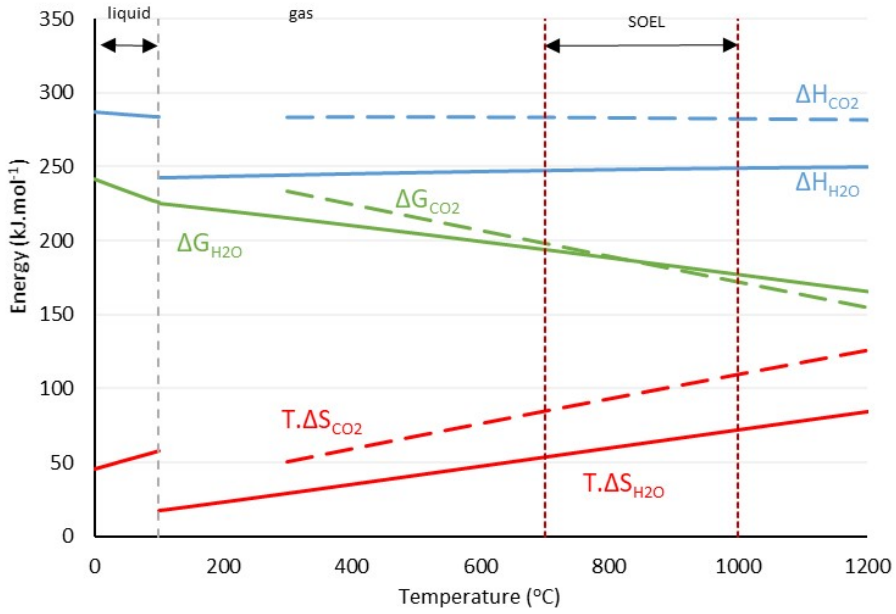

Figure 2.3: Stoichiometric energy demand for electrolysis of H_2O and CO_2 as a function of temperature [11].

One might now easily just think that the best option is to run the electrolysis on a temperature as high as possible to minimize the electricity demand. But, fact is that the heat must also come from somewhere. Therefore, SOEC has its main overall energy demand advantage over LTE only when high temperature heat is available from other external processes [11]. That is why both projects A and B introduced waste heat integration when using SOEC combined with steel production [8] [11]. By doing so, project A showed that the primary energy demand to produce steel can be reduced by 12.4 % if using SOEC compared to LTE [8]. After this, project B obtained a further improved number of 21 % [11]. Of importance is that the energy demanding vaporization step of water can be avoided if the DRP outlet gases are recycled directly into the SOEC again, something that is not possible when using LTE. Another profit is that the still large amounts of H_2 and CO in the DRP outlet gases don't have to be produced again from H_2O and CO_2 in the SOEC, requiring more electricity [8] [11]. Additionally, project B presented a cost analysis showing that the production costs of steel are likely to get lower for SOEC than LTE, if future investment cost targets for SOEC are reached. But for now, the cost is quite similar despite the SOEC system being more energy efficient [11].

Electrolysis at the high temperatures used in SOEC is a relatively new technology. It is proven on industrial scale, but it is not yet that implemented. One of the market leaders in electrolysis, Sunfire, manufactures a SOEC that can produce 750 Nm^3/h of syngas at various H_2:CO ratios. It is easy to scale by adding more modules together. Its

electrical efficiency is reported to be 82 % based on LHV [20]. Of an ideal SOEC system (without losses), the overall electrical efficiency including water evaporation is limited to 84.6 % based on LHV [29]. Another of the market leaders in electrolysis, Haldor Topsoe, mentions a conversion rate of at least 90 % in their SOEC if the temperature is increased by 30-50 °C [30]. With this, it is meant that the outlet gas temperature becomes higher than the inlet, because some extra electricity is added than what is needed purely thermodynamically seen. Thus, the SOEC can also work like a common electrical heater. A possible conversion rate of 80-90 % is further confirmed by Mougin et al. [31]. Anyway, project B used an electrolyzer efficiency of only around 70 % in its modeling [11].

2.4.1 Electrical Heating

In figure 2.4, a T-Q-diagram of an electrical heater is shown. If the temperature increase ΔT is 30 °C, a common TTD value is 5 °C [32]. The efficiency η of an electrical heater can be obtained with

$$\eta = \frac{\Delta T - \text{TTD}}{\Delta T}. \tag{2.15}$$

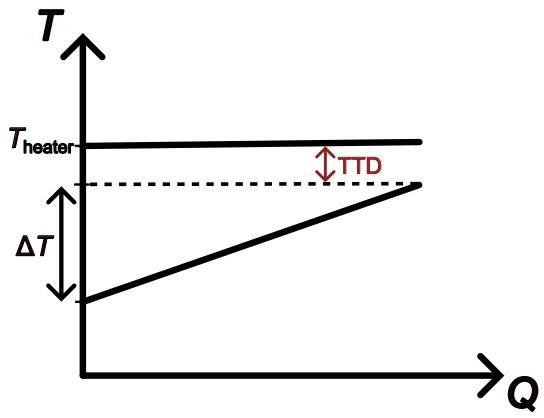

Figure 2.4: T-Q-diagram of an electrical heater.

2.5 SMR

SMRs are smaller nuclear power plants within the range of 10-300 MWe output. Their smaller scale and modular design aim to solve at least some of the challenges with new builds of conventional larger nuclear power plants, such as high cost and overrunning schedules [33]. However, as mentioned in the delimitations (section 1.3), this project did not dig deeply into the possible advantages with SMRs compared to conventional nuclear power plants. For such an analysis, also including description of various

reactor technologies, see e.g. Hagert and Blomgren [34] or the extensive *Handbook of Small Modular Nuclear Reactors* [33]. This work will now continue with its focus on investigating the possibilities of supplying steel industry with energy from SMRs.

There are many vendors and designs of SMRs. Some have reached further in their development than others. The SMR timeline indicates that demonstration of the first SMRs could take place in the mid to late 2020s, having commercial units in place mid-2030s [34]. As mentioned, this work will only consider technologies that are very likely to be on the market before 2035. Besides, as the DRP and the SOEC require very high temperatures, it would be advantageous out of an energy supply perspective if the SMR produces a very high temperature. Out of the so far most developed SMRs (likely to be on the market before 2035) are Chinese HTR-PM and American Xe-100 the two reactors that have the highest outlet temperature. Both are gas cooled and have an helium outlet temperature of 750 °C. They are roughly of the same size [35]. However, as this thesis is written in a western country, its continuing focus will lie on the American Xe-100.

2.5.1 Xe-100

The Xe-100 SMR from X-energy has a 200 MWth power per module. It is designed to come in a group of four modules together. It is a pebble bed reactor cooled by helium gas. Its basic design development was completed in 2021, resulting in applications submitted to the U.S. Nuclear Regulatory Commission the same year, hoping for a construction start in 2025 [35]. Further parameters as specified by X-energy [36] are gathered in table 2.2. Also their steam and turbine parameters are included. This is because the helium is heat exchanged with water in order to generate hot steam that afterwards is sent to turbines.

Table 2.2: Xe-100 parameters [36].

Construction start	2025
Thermal power	200 MW
Outlet He temp	750 °C
Inlet He temp	260 °C
He flow rate	71.1 kg/s
Inlet He pressure	60 bar
Steam temp	565 °C
Steam pressure	165 bar
Turbines' thermal efficiency	Up to 42.3 %

2.5.2 Turbines

The steam temperature is certainly set to 565 °C because it is a standard temperature used for steam turbines today. But as mentioned, both the DRP and the SOEC require even higher temperatures. A steam temperature of 650 °C is some kind of a maximum today if the turbines are to be of reasonable price. Otherwise, there is a need for super expensive materials, e.g. nickel, in the turbines. In year 2035, that value has most likely reached up to 670 °C. In addition to that, around 670 °C is actually the maximum steam temperature possible to obtain from the 750 °C helium. Regarding the steam pressure, values of up to 200 bar are possible for steam turbines [32].

Turbines are often composed together as a sequence starting with HPT and ending with LPT, including drainings in between. The turbines' thermal efficiency of up to 42.3 %, see table 2.2, is the overall efficiency for such a sequence of turbines.

A BPT can be used to produce power while lowering the pressure of a steam pipe. It is an isentropic process, with an isentropic efficiency η_S of around 88 % [32]. For an isentropic process going from state B to state A, it holds that

$$\eta_S = \frac{H_B - H_A}{H_B - H_{A,S}} \tag{2.16}$$

where $H_{A,S}$ can be obtained from REFPROP by using p_A and the same entropy as of state B. Now when H_B, $H_{A,S}$ and η_S are known, H_A can be obtained from the equation.

2.5.3 Pump

A pump operates in the opposite way to a turbine; by adding energy in the form of electricity it can increase the pressure in a pipe. It is necessary to pressurize the feedwater used to produce the hot steam obtained from heat exchanging with the helium gas reactor coolant. The electricity demand el_{pump} of a pump is calculated by

$$el_{pump} = \frac{\dot{m} dp}{\rho \eta} \tag{2.17}$$

where $\dot{m}$ is the mass flow through the pump, dp the pressure increase, ρ the density of the fluid and η the pump's efficiency. A common efficiency value of a pump used for nuclear power plants' feedwater supply is 85 % [32].

Chapter 3

The Proposed System Design

3.1 Method

Knowing that the DRP, SOEC and Xe-100 SMRs were to be the three main parts of the nuclear ironmaking system, the remaining parts as well as the connections between everything were established in order to come up with a detailed proposal of system design. Again, aiming for reducing the primary energy demand of fossil-free steel production by using direct heat integration of hot SMR steam into the process in a beneficial way. At first, it was thought that the system design would be more of a linear system in its nature. Thus, that the SMR steam would be sent directly into the SOEC to be turned into H_2, then inserted into the DRP. However, as mentioned in sections 2.3 and 2.4, it was found to be advantageous to operate the DRP on syngas and to recirculate the DRP outlet gases. As such large amounts were found to optimally be recycled, it was investigated instead how the recirculated gases could be reheated from the SMR steam.

The system design was developed based on the numbers of e.g. temperatures from chapter 2. Note especially that it was based on the same DRP operating condition as in project B (see table 2.1) because this was the only syngas operated DRP model found that had specified enough data for it to be useful as a black box for the system modeling that took place later on in this project. Additionally, where needed to establish the design, assumptions of e.g. temperatures were made.

All of this, with basis in a schematic of the proposed system design, is presented in the following result section 3.2. Then in chapter 4 comes the method and result of the system modeling, together with the modeling-related assumptions.

3.2 Result

Looking at the schematic in figure 3.1, it is seen that a mixture of H_2O, H_2, CO_2 and CO enters the DRP at 900 °C and 2 bar in pipe a. Using the project B model result, see table 2.1, the DRP outlet gas mixture in pipe b is at 464 °C and 1 bar [11]. The very small amount of CH_4 in pipes a and b, 0.14 mol %, is neglected and the sum of mol% is always normalized up to 1. Then 90 % of pipe b is recycled directly into the SOEC again. 10 % is combusted to avoid accumulation of inert gases.

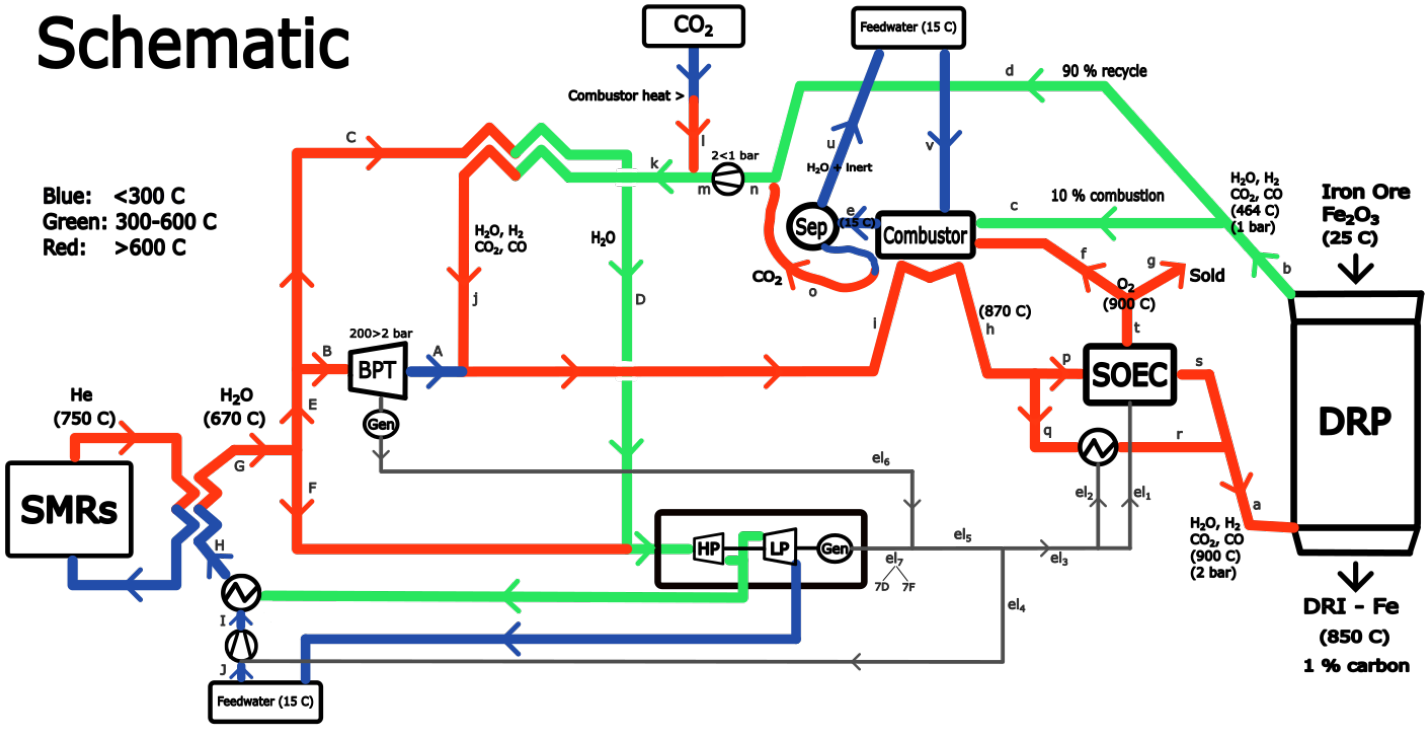

Figure 3.1: The schematic of the proposed system design.

The combustion of H_2 and CO occurs with O_2 taken from SOEC according to the reverse of reactions 2.IV and 2.V. The extra produced O_2 from SOEC can be sold. Totally complete combustion is assumed due to having excess of O_2 into the combustion. However, the products from the combustion are assumed to be only H_2O, CO_2 and inert gases, neglecting the 1 mol% of excess O_2 actually existing in pipe e according to project B [11]. As the combustion is highly exothermal the temperature has to be controlled in order to avoid temperature rises above material limits of around 1000 °C [32]. This is done by heat exchanging with pipe i-h (which in that way gets preheated into SOEC) and with external cold feedwater set to 15 °C. The purpose with the combustion is to be a preparatory step for separating out the inert gases (turning the four gases into two makes them easier to separate in the following step), meanwhile allowing for high temperature heat transfer to pipe i-h.

After combustion, the outlet pipe e is cooled all the way down to 15 °C. As the water content of pipe e is very high, it should be removed first through condensation [37]. The condensed water is then returned to the reservoir. 15 °C is a suitable temperature to reach down to for optimal condensation of water to take place. It is better to heat exchange with cold reservoir water than spraying water into the pipe e mixture to cool it, because if spraying, more CO_2 will dissolve into the water resulting in higher CO_2 emissions. But even though heat exchanging is the chosen method, some CO_2 emissions will occur with the condensed water [37]. After the condensation of water, the CO_2 and inert gases are left. It is possible to separate out pure CO_2 from that mixture, but it will cost some energy [37]. However, details regarding that separation process as well as its energy demand was dismissed from this work as it was not fully known which were the inert gases. Further research is needed.

Having reached after the separation processes, the CO_2 is to be returned to the recycled gases in pipe n. But first, the CO_2 is reheated with excess lower temperature (after pipe i-h heat exchanging has been finished) combustor heat. As it is preferable to compress at lower temperature, the mixture to be recycled is compressed in pipe n-m before heating takes place. This is to regain the desired inlet DRP pressure of 2 bar. CO_2 is added from a storage at 15 °C and 2 bar to replace the carbon that is added to the DRI. It can beneficially be bought from e.g. a large-scale DAC site or an industrial CCU site. Also this small amount of CO_2 is heated by the excess lower temperature combustor heat. Pipe k is heat exchanged with pipe C-D, thus benefiting from the hot SMR steam, to increase the temperature of the mixture that is to be sent into the SOEC. Note that the CO_2 is added before this heat exchanging to ensure that also this is further heated with the hot SMR steam.

Now looking at the 670 °C and 200 bar SMR steam, it is seen to be used in three ways. Firstly, as mentioned, via pipe C for heat exchanging the recirculated gases and then being sent into the turbines to produce electricity. Secondly, via pipe F for electricity production only. Thirdly, via pipe B to be added to the recirculated gases, replacing the water separated from the circuit via pipe u. Additionally, there is a BPT between pipes B and A to make use of the pressure drop by producing electricity. Note that the feedwater used to produce the SMR steam via heat exchanging with the 750 °C helium first is pressurized to 200 bar and then preheated by turbine drains.

As mentioned, pipe i-h is superheated by the combustor heat. It is controlled to reach 870 °C. However, when entering the DRP, pipe a is to have a temperature of 900 °C meaning that a 30 °C temperature increase in SOEC is used in this work. This has its basis in the SOEC numbers given in section 2.4, assuming that a 90 % conversion rate holds for a temperature increase of 30 °C. Because of using the 90 % value, while project B used 70 %, some amount has to only bypass the SOEC via pipe q-r (also heated 30 °C with an electrical heater) in order to meet the DRP inlet gas composition that is specified to be needed according to project B [11].

Chapter 4

Modeling of System

4.1 Method

Having the system design in place it was to be modeled in order to find out how much SMR steam that is needed to produce 1 ton of DRI. The modeling took place in Excel using data from REFPROP and was based on mass and energy balance calculations throughout the system (equations 2.2 and 2.3). In the end this means that for every pipe several parameters were known, including the energy content and amount of substance needed per ton DRI as well as the mixture's mol%, T, p and H. In addition to the assumptions needed to establish the system design, already presented together with the proposed system design in section 3.2, several modeling-related assumptions had to be made. Those are presented in this section along with the calculation descriptions.

In general, no pipe losses were assumed all over the system, both regarding mass and heat loss ($\dot{Q} = 0$ in equation 2.2). Isobar conditions were assumed for all processes except for the DRP, compressor, pump and turbines. That means that the Xe-100 outlet helium pressure was assumed to be the same as the inlet pressure of 60 bar, neglecting the small compressor work needed here. Looking at the schematic in figure 3.1, it can also be seen that the electricity demand of the compressor between pipes m-n was neglected. The same holds for any other (small) electricity demand that is not indicated with a cable in the schematic. Additionally, the energy demand of the CO_2 storage was neglected.

First out was the mass balance calculation throughout the system (only the lowercase letter pipes, see figure 3.1). The DRP inlet- and outlet gas molar flows and mol% from table 2.1 were used initially. Then from pipe b and onward started the quite simple mass balance calculations, following the resulting system design as explained in section 3.2. Apart from the assumptions in that section it needs to be mentioned that for the modeling, the loss of CO_2 via the condensed water in the separation process was neglected and set to zero. That means that the CO_2 added to the system in pipe l could be obtained as the difference in molar flow between pipe a (98.4 kmol/tDRI) and b (97.6 kmol/tDRI).

After this came the energy balance calculation. Knowing the molar content in every pipe needed to produce 1 ton of DRI, the energy content could be obtained by using equations

2.2 and 2.3, again starting in pipe b. The same reference point, with usage of $H = 0$ and $S = 0$ for $T = 25$ °C and $p = 1$ bar, was set to hold for every mixture and pure substance in REFPROP. Care was also taken for always using the same substance specific tabular for each gas in REFPROP. Some of REFPROP's standard tabulars had to be changed to allow for the very high temperature intervals needed in this modeling. Despite doing so, the enthalpy values for H_2 and CO of around 700 °C and above had to be extrapolated using the REFPROP built-in extrapolation.

Pipes o and l were in a first step assumed to be able to reach 600 °C with the excess lower temperature combustor heat. The calculations regarding the heat exchanging that occurs in the combustor are yet to be described in detail, as no iterative optimization was done of these two temperatures. The reader is left with that temperature assumption for now, having to see what it will result in later on. In that way, the energy content in pipe n was known. A constant temperature was assumed to hold when passing the n-m compressor. Indeed, a more rigorous compressor calculation would have been a polytropic process with an efficiency of about 0.88 [32], but that was not made here as the pressure difference is small.

Reaching the k-j vs C-D heat exchanger, equation 2.13 was used with the assumption of that the commonly used efficiency value of $\eta = 90$ % holds for all types of fluid mixtures. $C_{p,\mathrm{cold}}$ and $C_{p,\mathrm{hot}}$ were assumed to be the C_p values of the inlets k and C respectively, as the temperatures needed to obtain the C_p values of the outlets were still unknown. In this way, an iterative process could be avoided. As there were three unknowns, T_j, T_D and $\dot{n}_\mathrm{hot}$, while equation 2.13 only gives two, it was rewritten to form the functions

$$T_\mathrm{j}(\dot{n}_\mathrm{hot}) = \frac{0.9 \min(\dot{n}_\mathrm{cold} C_{p,\mathrm{k}},\ \dot{n}_\mathrm{hot} C_{p,\mathrm{C}})\ (T_\mathrm{C} - T_\mathrm{k})}{\dot{n}_\mathrm{cold} C_{p,\mathrm{k}}} + T_\mathrm{k} \tag{4.1}$$

$$T_\mathrm{D}(\dot{n}_\mathrm{hot}) = \frac{-0.9 \min(\dot{n}_\mathrm{cold} C_{p,\mathrm{k}},\ \dot{n}_\mathrm{hot} C_{p,\mathrm{C}})\ (T_\mathrm{C} - T_\mathrm{k})}{\dot{n}_\mathrm{hot} C_{p,\mathrm{C}}} + T_\mathrm{C}. \tag{4.2}$$

Starting with function 4.1, the only dependence of $\dot{n}_\mathrm{hot}$ is within the min function. As it is desired to obtain T_j as high as possible, in order to benefit maximally from the SMR steam for heating the recirculated gases, $\dot{n}_\mathrm{hot}$ was obtained from the tipping point of the min function, where equality holds. In that way, T_j gets as high as possible without sending unnecessarily high amounts of SMR steam through the heat exchanger. By inserting that value of $\dot{n}_\mathrm{hot}$ into equations 4.1 and 4.2, it holds that $T_\mathrm{j} = 650.25$ °C and $T_\mathrm{D} = 492.27$ °C.

For the BPT, equation 2.16 was used together with its surrounding methodology description straight away in order to obtain the enthalpy of pipe A, H_A. Using that also the flow of pipe A-B was known from before (set equal to pipe u flow), the temperature of pipe i was obtained to $T_\mathrm{i} = 612.90$ °C.

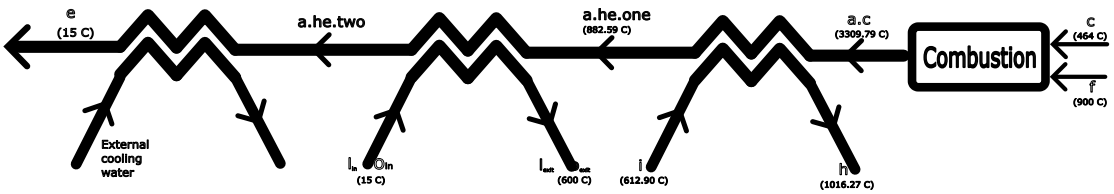

Figure 4.1: The modeling of the combustion process.

The combustion process was modeled as depicted in figure 4.1. In a first step, the chemical reactions were assumed to take place without cooling, allowing for the temperature to reach the adiabatic combustion temperature $T_{\text{a.c.}}$. This step was calculated such that the reactants were assumed to be cooled down to the reference state where the reaction then occurs, as the combustion temperature was unknown. Thus, the excess overall enthalpy from the reactions, $H^{\text{tot}}_{\text{reaction}}$, was calculated as

$$H^{\text{tot}}_{\text{reaction}} = \sum_{\text{reactants}} \left(\int C_p dT \right) + H^{0}_{\text{F,products}} - H^{0}_{\text{F,reactants}} \tag{4.3}$$

for the combustion of H_2 and CO respectively. Those were multiplied with the molar content of H_2 and CO in pipe c, respectively, (similarly to as in equation 2.3 but with molar based enthalpy values) to obtain their energy content after combustion. A combustion thermal efficiency of 98 % was accounted for. Lastly, the existing energy content of the inlet amounts of H_2O and CO_2 was added to obtain the total amount of energy available at state a.c. $Q^{\text{tot}}_{\text{a.c.}}$. From this, first $H^{\text{tot}}_{\text{a.c.}}$ and then $T_{\text{a.c.}}$ = 3309.79 °C could be obtained.

In a second step, the first heat exchanging was assumed to occur with pipe i-h. There were only two unknowns, the outlet temperatures, so equation 2.13 could be used right away resulting in T_{h} = 1016.27 °C and $T_{\text{a.he.one}}$ = 882.59 °C. In a third step came the reheating of the CO_2 in pipes o and l, which prior to these calculations had been assumed to reach 600 °C from this heat exchange. As can be seen in figure 4.1, T_{o} and T_{l} could have been assumed a bit higher also considering their flow rate being smaller than the combustion flow, but that was not optimized further. The flows in pipe o and l are very small anyway. In a fourth step came the cooling with external feedwater, so that the temperature in pipe e reached the desired 15 °C allowing for the water to condense.

The most important outcome of this combustor calculation, including its related heat exchangers, was that the obtained T_{h} = 1016.27 °C got higher than the desired 870 °C. This is important, because in reality the temperature must be controlled along the way so that $T_{\text{a.c.}}$ cannot be reached. That results in less quality heat being able to be transferred to pipe i-h. In this work, the assumption was made that as a higher temperature was obtained in these calculations, it is seen as very likely that the desired temperature of 870 °C can be reached even under the restrictions of reality. By this conclusion, the heat balance calculation was considered as complete. The amount of steam needed for heat integration per ton DRI, pipe E, had been found and heat balance had been proven throughout the system.

What remains is the electricity balance calculation. In reality, the heating in SOEC takes place meanwhile the reactions occur, but here it was assumed that all of the reactions occur at the mean temperature of 885 °C. For that reaction state, molar based $\Delta G^{885°C,\ 2bar}$ values of both H_2O and CO_2 electrolysis (reactions 2.IV and 2.V) was calculated stoichiometrically by following equations 2.6 and 2.7. Having that in place, the electricity demands of H_2O and CO_2, el_{H_2O} and el_{CO_2}, were obtained as

$$el_{H_2O} = 0.9\, n^{p}_{H_2O} \frac{\Delta G^{885°C,\ 2bar}_{H_2O}}{0.846} \tag{4.4}$$

$$el_{CO_2} = 0.9\, n^{p}_{CO_2} \frac{\Delta G^{885°C,\ 2bar}_{CO_2}}{0.846}, \tag{4.5}$$

accounting for that only 90 % of the molar flows of H_2O and CO_2 in pipe p, $n^{p}_{H_2O}$ and $n^{p}_{CO_2}$, gets converted and using the electrical efficiency value of 84.6 % found from section 2.4. The mixture to be heated was assumed to be the same as the mixture in pipe h, thus that no conversion had occurred yet. Thus, the electricity demand of the electrical heating from 870 °C to 900 °C, $el_{heating}$, was calculated as

$$el_{heating} = \frac{Q^{900°C}_{h} - Q^{870°C}_{h}}{\eta}, \tag{4.6}$$

where $\eta = 0.83$ was obtained by usage of TTD = 5 °C in equation 2.15.

As the BPT was seen as an isentropic process, its electricity production was simply calculated as the difference in energy content between pipe B and A. The electricity production from the chain of HPT and LPT was obtained as

$$el_{7D} = 0.423\, n_D\, (H_D - H_H) \tag{4.7}$$

$$el_{7F} = 0.423\, n_F\, (H_F - H_H) \tag{4.8}$$

for the steam content in pipe D and F respectively, using molar based enthalpy values and X-energy's specified turbines' thermal efficiency of up to 42.3 % from table 2.2. That efficiency was interpreted to be seen as the thermal efficiency for a control volume consisting of turbines, pump and preheater. Thus, the heat for preheating lost from turbine drains and the electricity demand of the pump was interpreted to be included in that value. Furthermore, it was assumed that the energy demand for pump and preheater can be covered exactly by using that value, even though the inlet temperature to the turbines is lower than the X-energy specified value of 565 °C.

Apart from this, one must note that the amount of steam that does not go through the HPT and LPT, but is inserted directly into the recirculated gases via pipe B-A, had to be handled in a special way as its energy demand for preheater and pump is not produced within the control volume. Therefore, the pump's electricity demand for that flow was calculated using equation 2.17 and added to the total demand via el_4 in figure 3.1. The

heat for preheating that flow was assumed to be taken from somewhere in the system where low temperature heat is available.

At the end, the electricity flows el_5, el_6 and el_{7D} were known per ton DRI. From this, the electricity demand to be produced from pipe F, el_{7F}, could easily be obtained. By knowing that, the steam needed in pipe F was found by using equation 4.8. Thus, the remaining part of the SMR steam demand per ton DRI had been determined.

In order to be able to scale the resulting SMR steam demand per ton DRI, the helium to steam heat exchanger had to be modeled. A T-Q-diagram of that heat exchanger is seen in figure 4.2. As the boiling temperature of water at 200 bar is 365.75 °C it means that this heat exchanging occurs while the water undergoes heating, boiling and superheating until it reaches the desired 670 °C. As mentioned around figure 2.2, for this case of heat exchanging the TTD number is often used. In this work, TTD = 10 °C was assumed [32]. By assuming that, the enthalpies at states 1,2,3 and 4 were known. Then equation 2.14 was used such that

$$\dot{n}_{\mathrm{He}}\,(H_1 - H_2) = \dot{n}_{\mathrm{H_2O}}\,(H_3 - H_4), \tag{4.9}$$

from which the steam flow rate for one SMR reactor, $\dot{n}_{\mathrm{H_2O}}$, became the only unknown as the helium flow rate for one SMR reactor, $\dot{n}_{\mathrm{He}}$, had already been specified in table 2.2. The obtained steam flow rate for one SMR reactor could then be compared with the steam needed to produce 1 ton of DRI in order to perform real scale result analysis.

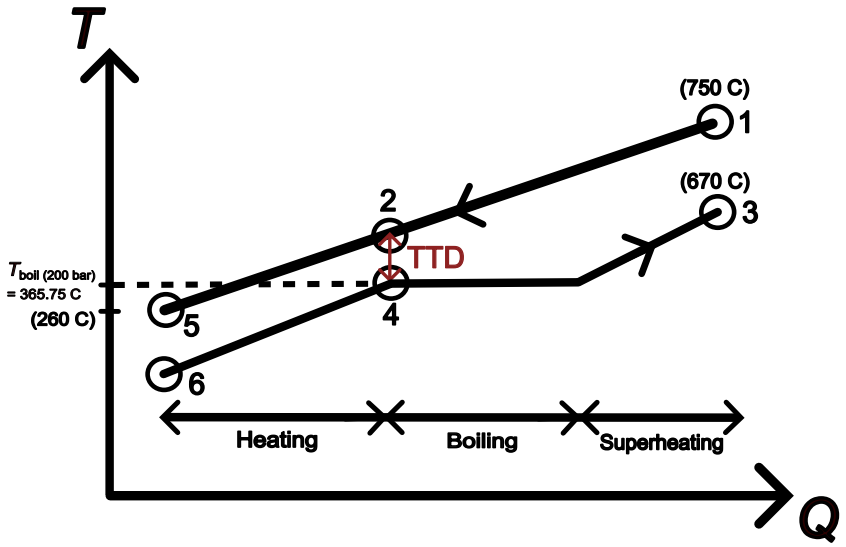

Figure 4.2: T-Q-diagram of the SMR helium to steam heat exchanger.

4.2 Result

With this proposed system using direct heat integration of hot SMR steam into the fossil-free steel production process, 7.0 MWh of steam is needed per ton DRI. More specifically, that is the total amount of steam needed (pipe G in figure 3.1) to supply the system of DRP and electrolysis with energy. HYBRIT specifies that 3.2 MWh of electricity is needed per ton DRI for the same system boundaries (DRP and electrolysis) of their system running on LTE without direct or waste heat integration [38]. If calculating how much SMR steam that would be needed only to produce that amount of electricity, to be able to make comparisons in the same energy form, it would be 10.9 MWh of SMR steam. Thus, the proposed SMR-integrated system shows a reduction in energy demand of 36 % compared to the HYBRIT system.

Table 4.1: Energy demand of the proposed vs the HYBRIT system.

Steam demand of the proposed system	7.0 MWh/tDRI
Steam demand of the HYBRIT system	10.9 MWh/tDRI
Reduction	36 %

To see these results in a larger perspective some scaling is needed. The scaling is based on Sweden's mining of iron ore, 29.2 Mton in 2020 [4]. If all of that was turned into DRI, it would correspond to a DRI production of 21 Mton DRI per year (by using that one ton of iron ore leads to 0.66 ton steel [11] and that one ton of DRI is 0.93 ton steel [39]). That means that with the proposed system, 64 Xe-100 SMRs would be needed to run constantly with 100 % deliverability to supply the Swedish DRI production with energy. If only producing electricity, these SMRs would be able to produce 43 TWh of electricity per year.

1.7 % of the SMR steam flows through pipe B (see figure 3.1) to be added to the recycled gases and 17.5 % flows through pipe C to reheat the recycled gases. Thus together, 19.2 % of the SMR steam is used for direct heat integration (pipe E in figure 3.1). That corresponds to 12 out of the 64 SMRs. Then 80.8 % is used for electricity production only (pipe F), corresponding to 52 SMRs.

Table 4.2: The amount of Xe-100 SMRs needed to supply the energy demand of Sweden's DRI production with the proposed system.

In total	64 SMRs
For direct heat integration	12 SMRs
For electricity production	52 SMRs

Chapter 5

Discussion

5.1 Energy Demand and Supply for DRI Production

First of all, the obtained result of a 36 % reduction in primary energy demand per ton DRI for the proposed SMR-integrated system compared to the HYBRIT system (see table 4.1) needs to be commented. Again, the proposed system uses SOEC with direct heat integration of hot SMR steam, waste heat integration and by-product utilization while the HYBRIT system uses LTE and electrical heating. In section 2.4 it was written that project A and B showed a 12.4 % or 21 % reduction respectively if using SOEC with waste heat integration and by-product utilization compared to using LTE and electrical heating. By those means it can be seen as proven that the remaining aspect, direct heat integration of hot SMR steam, reduces the energy demand even further. But of course the different projects have used somewhat unsimilar assumptions, system boundaries etc in their models. Such are not clearly specified together with the energy demand found for the HYBRIT system. However, this work has large similarities with project B, while smaller with project A, for instance regarding unsimilar rates of carburization in the DRI product. That turns comparisons of the 36 % reduction value with the 21 % reduction value from project B into the more viable option, where direct heat integration can be seen as what makes the difference. This result is very interesting, not least as it is what this project initially was hoping for.

As mentioned, the perspective of being able to store energy in the form of hydrogen makes fossil-free steel production fueled by RES an interesting option, as hydrogen energy storage can help with providing grid stability in an energy system having large shares of intermittent RES. But apart from hydrogen production using electrolysis, the energy demand of most parts within the fossil-free steel production system is more constant in its nature. That holds particularly for the large energy demand of heating the DRP inlet gases to 900 °C. The question is where that enormous load is to come from when the intermittent RES don't produce electricity. This is of course another advantage with running the steel industry on high temperature SMR steam.

5.2 Simplification Analysis

When starting the project it was thought that apart from the SMR steam used only to produce electricity, most of the steam would be inserted directly into the SOEC (pipe B in figure 3.1) to produce H_2, which then was thought to be inserted into the DRP in a more simple linear process. But as seen from the result in section 4.2 only 1.7 % is inserted directly into the SOEC, while 17.5 % is used to reheat the recycled gases. This is the case due to that only 30 % of the H_2 and CO reacts in the DRP, making it favorable to recirculate the outlet DRP gases as then large amounts of H_2 and CO don't have to be produced again in the SOEC requiring energy. That fact makes also the system design an interesting result itself. However, that the outlet gases were found to optimally be recycled turned this modeling into a tougher work, resulting in the need for assumptions and simplifications, e.g. regarding that no optimization was performed in the modeling.

The EL-DRP-EAF route is a new area of research meaning that there are few available data. The individual components of the proposed system had often data for only one specific operating condition, making them hard to integrate into the system in the optimal way. That holds e.g. for the DRP, where only project B provided enough data in its modeling for it to be useful as a black box within this work. It is likely that the DRP operating condition used in that model has been optimized for the overall system it is integrated in, meaning that maybe another DRP operating condition would have been better for this work. But many factors within the operating condition of the DRP are anyway independent of the surrounding system in some ways. An example is the H_2:CO ratio. A ratio between 1.6 and 2.6 is optimal for the reduction rate of the iron ore, whereby project B simply used a ratio of 2.0 in its work. And again, the aim of this work was not to contribute with another thorough DRP modeling, but to analyze the possibilities of integrating SMRs with steel production.

When using equation 2.13 in the modeling, the C_p values were taken from the inlets as the outlet temperatures needed to obtain the outlet C_p values were unknown. A more precise modeling of the heat exchangers would have been to take the mean of the inlet and outlet C_p values, but to do so an iterative process would have been needed and that was considered as too complex and time consuming for the scope of a master thesis. This simplification has definitely affected the result, especially in the first heat exchanger of the combustion process (with pipe i-h, see figure 4.1) as the temperature difference is very large there. Thus, the difference between the inlet and outlet C_p values is considerable. For the combustion outlet flow, C_p = 61.366 kJ/kmolK at the first heat exchanger inlet of 3309.79 °C and C_p = 47.521 kJ/kmolK at the outlet of 882.59 °C. Additionally, the choice of only setting the CO_2 temperature in pipes o and l to 600 °C and not optimizing it further up with an iterative method has lowered the calculated overall efficiency to a small extent.

If more factors would have been included in the modeling, e.g. the delimitation of the small H_2 storage that is needed between the SOEC and DRP as well as the neglections of

pipe losses and CO_2 storage energy demand, the resulting energy demand of this system would be enlarged. However, the delimitations and neglections made of such factors can be considered as small compared to the overall energy demand. But of course it is somewhat energy demanding, e.g. in the small H_2 storage where the H_2 needs to be cooled down and then reheated again as it is too space demanding to store H_2 at such high temperature.

5.3 Using This System Model in the Steel Market

It is problematic that pelletizing, ironmaking and steelmaking are often not located in the same place, as that is of importance if aiming for obtaining the maximum performance out of a full nuclear steelmaking system. Only if all parts are in the same location the hot SMR steam can be beneficially used everywhere. Additionally, that makes it possible to reuse process heat between the different steps, such as sending hot iron ore pellets directly from the pelletizing process to the DRP. This work put its focus only on the DRP, but if e.g. the pelletizing and the DRP were to be located in the same place, the DRP inlet iron ore temperature should have been chosen higher than 25 °C. That would have reduced the energy demand needed to be supplied via the DRP inlet reduction gases and thus the energy demand of SMR steam. However, it would not have been very easy to analyze with this system modeling as then an own DRP model of another operating condition would have been needed. In the contrary, an EAF making direct usage of the 850 °C DRI by being in the same location could easily have been added to this system, but that was not done due to delimitations. If this system model was to be used for the case where the DRI is sold to another company producing the steel, the outlet DRI should be cooled while making usage of that heat within the system. In that case, the primary energy demand of the modeled system would be lowered.

In addition, thinking of that the DRI often would be sold, it is seen as a marketing advantage to have the carbon addition already in the DRP from CO just like in the proposed system. If the CO is produced of CO_2 coming from either DAC or CCU, the DRI-producing company can say that they take responsibility for that the carbon addition is performed in a fossil-free way storing otherwise atmospheric CO_2 into the product, as buying companies could add carbon from fossil sources instead. There is also a technical advantage that makes the DRI easier to sell as today's already existing EAFs are built for operating on carbon-containing iron. Furthermore, operating the EAF on carbon-containing iron reduces the electricity demand of the EAF.

5.4 Real Scale Integration of SMRs with Steel Industry

Ending the discussion comes an analysis of the scaled results, found in table 4.2, in order to answer the last remaining research question: ”In what ways could SMRs be reasonably integrated with the steel industry in a real scale?”. The number of 64 Xe-100 SMRs of 200 MWth power needed to supply the Swedish DRI production with energy is vast. It corresponds to 3.9 conventional nuclear power plants of 3.3 GWth power each. Additionally, as mentioned if only producing electricity all these SMRs would be able to produce 43 TWh of electricity per year, which can be compared to the total electricity production in Sweden of 166 TWh in 2021. It can be concluded that the energy demand is super large, but one should ask oneself: Is it really reasonable with 64 new SMRs in one place? One must also consider the problematic aspect of that the SMRs have to be placed in close connection to the existing steel industry locations, often being located close to cities, in order for the direct heat integration to function.

Therefore, it could be interesting to show how many SMRs that would be needed for direct heat integration only, because fact is that the direct heat integration is the main advantage with the proposed system leading to the reduction of primary energy demand. Then the electricity needed in addition could actually come from anywhere. As seen in table 4.2, only 12 SMRs are used for direct heat integration, a number which is much more likely to get allowance for constructing. Then the remaining electricity demand could be taken from the grid, produced by RES or more distant, maybe larger, conventional nuclear power plants with better possibilities of choosing the optimal locations for. This possibly more reasonable suggestion of 12 SMRs can be seen as a new way of thinking regarding nuclear energy; for heat integration only, leading to overall system energy efficiency advantages. Lots of fossil free energy of all kinds will be needed in the future and this suggestion allows for a mix of energy sources for its supply.

Lastly, considering the energy demand being that great it could have been more suitable to supply it with larger nuclear power plants instead of that many SMRs. As mentioned, there has been some projects going on earlier, especially in Japan, regarding supplying the steel industry with nuclear energy from VHTR. However, as today’s development focus of nuclear reactors lies mainly within the subject of SMRs, these were chosen to constitute the core of this study.

Chapter 6

Conclusion and Future Work

6.1 Conclusion

In this study it was investigated if it is possible to reduce the primary energy demand of fossil-free steel production according to the EL-DRP-EAF route by using direct heat integration of hot SMR steam into the process. To acheive this, a beneficial design of such a system was proposed, containing Xe-100 SMRs, SOEC and DRP as its main parts. The pelletizing and EAF were demarcated. Carbon was added to the DRI via operating the DRP on syngas. Having the system design in place, it was modeled in order to find out how much SMR steam that is needed to produce 1 ton of DRI. It was found that the primary energy demand of fossil-free steel production can be reduced when compared to other systems, with direct heat integration of hot SMR steam as what makes the difference. Though, that result is sensitive to somewhat unsimilar assumptions and system boundaries used in the compared models. Scaling of the result was performed based on the Swedish DRI production rate. As the energy demand is vast, the suggestion was made that SMRs could be used for direct heat integration only, whilst the remaining energy demand in the form of electricity could be taken from the grid. This was seen as a new way of thinking regarding nuclear energy; for heat integration only, allowing for a mix of energy sources but still leading to the energy efficiency advantages.

6.2 Future Work

This work could also be performed out of emission and cost perspectives, perhaps together with a further investigation of separation technologies to minimize the CO_2 emissions via the condensed water. Depending on the rate of CO_2 being dissolved in the water it might be preferable to heat the condensed water once again after condensation, as then the CO_2 dissolved in the water will evaporate.

New studies could be extended to include more parts of the EL-DRP-EAF route, e.g. the EAF, to see what advantages that might come by benefiting from SMR steam also there.

This work could be made more thoroughly with a more complex modeling of the system, based on an iterative optimization. An own detailed DRP modeling could be included. By doing that, it could be investigated what the optimal DRP operating condition for this system is, leading to an improved performance. Furthermore, the desired carburization rate of 3-4.5 % in the DRI product and not 1 % could be used.

It would be interesting to compare different possible technologies of carbon addition to the final steel product, including a nuclear driven pyrolysis. Nuclear very high temperature steam can be used to run a steam pyrolysis, where biomass is disintegrated into biogas, biooil and biocoal. This work used CO as a reductant in the DRP so that carbon is added to the DRI, but as mentioned, it is also possible to use biocoal in the EAF so that carbon is added to the final steel product. Thus, the biocoal produced from pyrolysis could be used for carbon addition in the EAF and the biogas and biooil could be sold.

A further comparison to this study could be made by investigating integration of other nuclear reactors. That could be larger scale reactors, bearing the large energy demand in mind. Additionally, it would be of interest to see studies analyzing how even higher temperature reactors, thinking of the 950 °C helium outlet temperature from the Japanese VHTR, could lead to an improved overall energy efficiency. As SOEC was not used in the former Japanese studies of integrating VHTR in steel production, such studies would still be something new. Perhaps even the helium could be used to reheat the recirculated gases directly, having to go through only one and not two heat exchangers from helium to steam to recirculated gases.

Bibliography

[1] IPCC, 'Summary for policymakers. In: Climate Change 2022: Mitigation of Climate Change. Contribution of working group III to the sixth assessment report of the intergovernmental panel on climate change,' *Cambridge University Press*, 2022.

[2] M. Fischedick, J. Marzinkowski, P. Winzer and M. Weigel, 'Techno-economic evaluation of innovative steel production technologies,' *Journal of Cleaner Production*, vol. 84, pp. 563–580, 2014, ISSN: 0959-6526. DOI: 10.1016/j.jclepro.2014.05.063.

[3] A. Bhaskar, M. Assadi and H. Nikpey Somehsaraei, 'Decarbonization of the iron and steel industry with direct reduction of iron ore with green hydrogen,' *Energies*, vol. 13, no. 3, 2020, ISSN: 1996-1073. DOI: 10.3390/en13030758.

[4] World Steel Association. 'World steel in figures 2022.' (2022), [Online]. Available: https://worldsteel.org/wp-content/uploads/World-Steel-in-Figures-2022.pdf (visited on 10/08/2022).

[5] IEA. 'Iron and steel.' (2021), [Online]. Available: https://www.iea.org/reports/iron-and-steel (visited on 10/08/2022).

[6] Naturvårdsverket. 'Industri, utsläpp av växthusgaser.' (2022), [Online]. Available: https://www.naturvardsverket.se/data-och-statistik/klimat/vaxthusgaser-utslapp-fran-industrin/ (visited on 11/08/2022).

[7] EUROFER. 'What is steel and how is steel made?' (2020), [Online]. Available: https://www.eurofer.eu/about-steel/learn-about-steel/what-is-steel-and-how-is-steel-made/ (visited on 11/08/2022).

[8] N. Müller, G. Herz, E. Reichelt, M. Jahn and A. Michaelis, 'Assessment of fossil-free steelmaking based on direct reduction applying high-temperature electrolysis,' *Cleaner Engineering and Technology*, vol. 4, p. 100 158, 2021, ISSN: 2666-7908. DOI: 10.1016/j.clet.2021.100158.

[9] M. Weigel, M. Fischedick, J. Marzinkowski and P. Winzer, 'Multicriteria analysis of primary steelmaking technologies,' *Journal of Cleaner Production*, vol. 112, pp. 1064–1076, 2016, ISSN: 0959-6526. DOI: 10.1016/j.jclepro.2015.07.132.

[10] V. Vogl, M. Åhman and L. J. Nilsson, 'Assessment of hydrogen direct reduction for fossil-free steelmaking,' *Journal of Cleaner Production*, vol. 203, pp. 736–745, 2018, ISSN: 0959-6526. DOI: 10.1016/j.jclepro.2018.08.279.

[11] A. Krüger, J. Andersson, S. Grönkvist and A. Cornell, 'Integration of water electrolysis for fossil-free steel production,' *International Journal of Hydrogen Energy*, vol. 45, no. 55, pp. 29 966–29 977, 2020, ISSN: 0360-3199. DOI: 10.1016/j.ijhydene.2020.08.116.

[12] HYBRIT. 'SSAB, LKAB and Vattenfall first in the world with hydrogen-reduced sponge iron.' (2021), [Online]. Available: https://www.hybritdevelopment.se/en/hybrit-ssab-lkab-and-vattenfall-first-in-the-world-with-hydrogen-reduced-sponge-iron/ (visited on 13/09/2022).

[13] SCB. 'Elproduktion och förbrukning i Sverige.' (2022), [Online]. Available: https://www.scb.se/hitta-statistik/sverige-i-siffror/miljo/elektricitet-i-sverige/ (visited on 13/09/2022).

[14] S. Axelsson, A. Pettersson, J. Moström and M. Källgren. 'Alla fossilfria energislag kommer behövas.' (2022), [Online]. Available: https://www.energiforetagen.se/pressrum/debattartiklar/2022/att-i-detta-akuta-lage-lasa-sig-vid-diskussioner-om-teknikval-skapar-osakerhet-for-saval-energibranschen-som-industrin-som-ar-i-behov-ny-fossilfri-el/ (visited on 13/09/2022).

[15] Y. Inagaki, S. Kasahara and M. Ogawa, 'Merit assessment of nuclear hydrogen steelmaking with very high temperature reactor,' *ISIJ International*, vol. 52, no. 8, pp. 1420–1426, 2012. DOI: 10.2355/isijinternational.52.1420.

[16] X. L. Yan, S. Kasahara, Y. Tachibana and K. Kunitomi, 'Study of a nuclear energy supplied steelmaking system for near-term application,' *Energy*, vol. 39, no. 1, pp. 154–165, 2012, ISSN: 0360-5442. DOI: 10.1016/j.energy.2012.01.047.

[17] L. Germeshuizen and P. Blom, 'A techno-economic evaluation of the use of hydrogen in a steel production process, utilizing nuclear process heat,' *International Journal of Hydrogen Energy*, vol. 38, no. 25, pp. 10 671–10 682, 2013, ISSN: 0360-3199. DOI: 10.1016/j.ijhydene.2013.06.076.

[18] S. Kasahara, Y. Inagaki and M. Ogawa, 'Process flow sheet evaluation of a nuclear hydrogen steelmaking plant applying very high temperature reactors for efficient steel production with less co2 emissions,' *Nuclear Engineering and Design*, vol. 271, pp. 11–19, 2014, ISSN: 0029-5493. DOI: 10.1016/j.nucengdes.2013.11.002.

[19] M. Ni, M. K. Leung and D. Y. Leung, 'Technological development of hydrogen production by solid oxide electrolyzer cell (SOEC),' *International Journal of Hydrogen Energy*, vol. 33, no. 9, pp. 2337–2354, 2008, ISSN: 0360-3199. DOI: 10.1016/j.ijhydene.2008.02.048.

[20] Sunfire. 'Sunfire Factsheet SynLink SOEC.' (2021), [Online]. Available: https://www.sunfire.de/en/syngas (visited on 23/09/2022).

[21] S. Nordgren, J. Dahl, C. Wang and B. Lindblom, 'Process integration in an iron ore upgrading process system – Analysis of mass and energy flows within a straight grate induration furnace,' *Czech Society of Chemical Engineering*, 2008.

[22] Private communication with Valentin Vogl, Doctoral student at Environmental and Energy Systems Studies, Lund University, 9th Sep. 2021.

[23] LKAB. 'Our strategy for the future.' (2022), [Online]. Available: https://lkab.com/en/what-we-do/our-strategy/ (visited on 14/09/2022).

[24] P. Atkins, J. de Paula and J. Keeler, *Atkins' Physical Chemistry*. Oxford University Press, 2017, ISBN: 9780198769866.

[25] P. Perrot, *A to Z of Thermodynamics*. Oxford University Press, 1998, ISBN: 9780198565529.

[26] Swiss Rotors. 'How do you calculate the efficiency of a plate heat exchanger?' (2020), [Online]. Available: https://swissrotors.com/blog/how-do-you-calculate-the-efficiency-of-a-plate-heat-exchanger/ (visited on 26/09/2022).

[27] L. Yi, Z.-c. Huang, H. Peng and T. Jiang, 'Action rules of H2 and CO in gas-based direct reduction of iron ore pellets,' *Journal of Central South University*, vol. 19, 2012, ISSN: 2291-2296. DOI: 10.1007/s11771-012-1274-0.

[28] SGU, 'Mineralmarknaden 2018 - Tema: Järn och stål,' *Periodiska publikationer*, vol. 2019, no. 1, 2019, ISSN: 0283-2038. [Online]. Available: http://resource.sgu.se/produkter/pp/pp2019-1-rapport.pdf (visited on 21/09/2022).

[29] A. Buttler and H. Spliethoff, 'Current status of water electrolysis for energy storage, grid balancing and sector coupling via power-to-gas and power-to-liquids: A review,' *Renewable and Sustainable Energy Reviews*, vol. 82, pp. 2440–2454, 2018, ISSN: 1364-0321. DOI: 10.1016/j.rser.2017.09.003.

[30] Private communication with Haldor Topsoe, 7th Oct. 2021.

[31] J. Mougin, S. D. Iorio, A. Chatroux *et al.*, 'Development of a solid oxide electrolysis stack able to operate at high steam conversion rate and integration into a SOE system,' *ECS Transactions*, vol. 78, no. 1, pp. 3065–3075, 2017. DOI: 10.1149/07801.3065ecst.

[32] Private communication with Magnus Genrup, Professor at Thermal Power Engineering and Department Head at the Department of Energy Sciences, Lund University, 8th Jul. 2022.

[33] N. Todreas, '1 - Small modular reactors (SMRs) for producing nuclear energy: An introduction,' in *Handbook of Small Modular Nuclear Reactors (Second Edition)*, ser. Woodhead Publishing Series in Energy, D. T. Ingersoll and M. D. Carelli, Eds., Second Edition, Woodhead Publishing, 2021, pp. 3–27, ISBN: 978-0-12-823916-2. DOI: 10.1016/B978-0-12-823916-2.00001-1.

[34] B. Hagert and L. Blomgren, 'Low-carbon hydrogen production using small modular reactors,' pp. 45–56, 2021. [Online]. Available: https://hdl.handle.net/20.500.12380/302478 (visited on 27/09/2022).

[35] IAEA, *Advances in Small Modular Reactor Technology Developments*. 2020. [Online]. Available: https://aris.iaea.org/Publications/SMR_Book_2020.pdf (visited on 27/09/2022).

[36] E. J. Mulder, 'Overview of X-Energy's 200 MWth Xe-100 Reactor,' *National Academy of Sciences*, 13th Jan. 2021.

[37] Private communication with Ola Wallberg, Professor and Department Head at the Department of Chemical Engineering, Lund University, 26th Aug. 2022.

[38] SSAB. 'SSAB, LKAB and Vattenfall to build a globally-unique pilot plant for fossil-free steel.' (2018), [Online]. Available: https://www.ssab.com/en/news/2018/02/ssab-lkab-and-vattenfall-to-build-a-globallyunique-pilot-plant-for-fossilfree-steel (visited on 06/10/2022).

[39] G. L. Dressel, 'Use of DRI in EAF's,' [Online]. Available: https://www.dresseltech.com/dripart4.pdf (visited on 16/09/2022).